C. elegans colony formation as a phase separation phenomenon

Yuping Chen
Stanford Medicine
James Ferrell Jr. (james.ferrell@stanford.edu)
Stanford University

Article

Keywords: C. elegans, phase separation, population density

Posted Date: July 24th, 2020

DOI: https://doi.org/10.21203/rs.3.rs-45159/v1

Version of Record: A version of this preprint was published at Nature Communications on August 16th, 2021. See the published version at https://doi.org/10.1038/s41467-021-25244-9.

Abstract

Phase separation at the molecular scale affects many biological processes. The theoretical requirements for phase separation are fairly minimal, and analogous phenomena may occur at other scales in biology. Here we have examined colony formation in the nematode C. elegans as a possible example of phase separation by a population of organisms. Experimental data and mathematical modeling indicated that, similar to physical condensation processes like phase separation and micelle formation, the population density of worms determines colony formation in a thresholded fashion, with the threshold correctly predicted by phase separation theory. Furthermore, we found that a phenomenon akin to Ostwald ripening – a coarsening seen in many systems that undergo phase separation – occurs. Our results show that populations of organisms can undergo condensation phenomena and phase separation.

Main Text:

Current studies of phase separation in biology have focused on the behaviors of microscopic molecular assemblies [1], including P granules [2], stress granules [3], and nucleoli [4]. Theoretical considerations show that the requirements for phase separation are fairly minimal; it would not be surprising if analogous phenomena were to occur at other scales in biology.

C. elegans is a macroscopic animal that exhibits chemotaxis [5], learning [6], and complex social behaviors [7,8]. It has been shown that some strains of *C. elegans* feed in clumps at the edges of existing bacterial lawns [9]. This social feeding behavior has been attributed to the sensing of local oxygen levels [10,11]. However, some strains, including the classic lab strain, N2 Bristol, lack the ability to clump in this fashion [9].

In the course of other studies, we observed what appears to be a particularly simple type of *C. elegans* colony formation: we found that N2 Bristol worms growing on plates to high density (a high number of worms per unit area), so that the bacterial food source was exhausted, often formed colonies (Fig. 1a). Recently, Demir *et al*. reported what appeared to be a related patterning behavior, and showed that it depended on bacteria [12]. To test if residual bacteria or a pre-deposited pheromone pattern is required for the colony formation we had observed, we washed and transferred adult N2 worms to a fresh agarose plate. In the absence of added bacteria, a high density (0.18 worms/mm^2) of adult worms formed colonies within minutes (Fig. 1c, Supplementary Movie 1), whereas a low density (0.01 worms/mm^2) did not (Fig. 1b, Supplementary Movie 2). Even after 12 h of incubation, low densities of worms did not form colonies (Supplementary Fig. 1). We also tested *C. elegans* at other developmental stages, including dauer and asynchronized stages. Notably, to obtain dauer worms, we washed and treated with a low dose of detergent before replating, which should lyse and eliminate any trace amounts of bacteria. As was the case with adults, worms in these developmental stages formed colonies at high density, but not at low density (Supplementary Fig. 2). Thus, a system consisting of worms alone, with no bacteria, can undergo

colony formation, and this colony formation depends upon the density of worms. Here we set out to see if this process can be viewed as a phase separation phenomenon.

On plates with colonies, we observed that worms dynamically moved into and out of the colonies (Supplementary Movie 3). In this way, the phenomenon resembled molecular liquid-liquid phase separation, as molecules also dynamically exchange between two phases. We asked if the formation of *C. elegans* colonies might be explained by phase separation theory. Typical theoretical approaches begin with expressions for the equilibrium energy or chemical potential of all of the species involved. However, phase separation phenomena can also be explored with rate equations, a complementary approach where rates, which can be directly determined by tracking experiments, rather than enthalpies and entropies, are the relevant species.

We defined two states or compartments for the worms, worms in a colony, w^*, and dispersed, solitary worms, w, and considered the processes that allow a worm to join or leave a colony (Fig. 2a). The worms' crawling grossly resembled a random walk [13] (Fig. 2b), and a log-log plot of mean squared displacement vs. time yielded a slope of $\alpha = 1.11 \pm 0.15$ (Fig. 2c), again consistent with a random walk. We therefore assumed that the worms approached colonies from random directions, and that the probability of an encounter between a worm and a colony was proportional to the perimeter of the colony. Note that if the worms' trajectories had been more ballistic (straight lines with few turns and $\alpha = 2$), the probability should be proportional to the cross-sectional diameter of the colony. In either case, the encounter rate should be proportional to the square root of the area of colonies, and the square root of the number of worms in the colony $w^{*1/2}$. The encounter rate should also be proportional to the number of out-of-colony worms, w. With these assumptions, the forward rate of the process can be expressed as:

$$\text{Forward rate} = k_1 w (w^*)^{\frac{1}{2}}, \qquad \text{[Eq 1]}$$

where k_1 is the rate constant for the process. The departure of worms from a colony should also be proportional to the square root of the area of colonies, $w^{*1/2}$. Hence, the reverse rate is:

$$\text{Reverse rate} = k_{-1} (w^*)^{\frac{1}{2}}, \qquad \text{[Eq 2]}$$

where k_{-1} is the reverse rate constant. The net rate of colony formation can thus be written as

$$\frac{dw^*}{dt} = k_1 w (w^*)^{\frac{1}{2}} - k_{-1} (w^*)^{\frac{1}{2}}. \qquad \text{[Eq 3]}$$

We assume that the total number of worms in the system is a constant w_{tot}, which means that:

$$w_{tot} = w + w^*. \qquad \text{[Eq 4]}$$

Therefore, Eq. 3 can be written as:

$$\frac{dw^*}{dt} = k_1(w_{tot} - w^*)(w^*)^{\frac{1}{2}} - k_{-1}(w^*)^{\frac{1}{2}}, \qquad \text{[Eq 5]}$$

with a single time-dependent variable (w^*). At steady state, the time derivative must equal zero:

$$0 = k_1(w_{tot} - w^*_{ss})(w^*_{ss})^{\frac{1}{2}} - k_{-1}(w^*_{ss})^{\frac{1}{2}}, \qquad \text{[Eq 6]}$$

where W^*_{ss} is the steady-state number of worms in the colony. There are two solutions for W^*_{ss}:

$$w^*_{ss} = 0, \qquad \text{[Eq 7]}$$

which means that there is no colony and all of the worms are dispersed and solitary, and:

$$w^*_{ss} = w_{tot} - {}^{k_{-1}}/_{k_1}. \qquad \text{[Eq 8]}$$

Note that neither W^*_{ss} nor w_{tot} can be smaller than zero. This means that there is a single steady state when $0 \leq w_{tot} \leq k_{-1}/k_1$—the steady state given by Eq. 7—and two steady states when $w_{tot} > k_{-1}/k_1$ (Fig. 2d, e)—the solutions to Eqs. 7 and 8.

To determine which of the steady states is stable, we performed rate-balance analysis (Fig. 2f, g). When $0 \leq w_{tot} \leq k_{-1}/k_1$, the single steady state, where $W^*_{ss} = 0$ and $w_{ss} = w_{tot}$, is stable (Fig. 2f). On the other hand, when $w_{tot} > k_{-1}/k_1$, there are two steady states, which include a stable steady state, where $W^*_{ss} = w_{tot} - k_{-1}/k_1$ and $w_{ss} = k_{-1}/k_1$, and an unstable steady state, where $W^*_{ss} = 0$ and $w_{ss} = w_{tot}$ (Fig. 2g). Thus, when w_{tot} is below a threshold value of $w_{tot} = k_{-1}/k_1$, no colony will form. And, when w_{tot} is above this threshold, a colony will form and increase in size as w_{tot} increases, with the density of the out-of-colony worms remaining at its maximal possible density of k_{-1}/k_1 (Fig. 2d - g). The transition from one to two steady states that occurs at $w_{tot} = k_{-1}/k_1$ is called a transcritical bifurcation [14]. Transcritical bifurcations are seen in simple models of micelle formation, liquid-liquid phase separation, and precipitation, various condensation processes that occur on a molecular level [15–17].

Note that so far we are considering the interplay between dispersed worms and a single colony. However, the analysis can easily be extended to multiple colonies (Supplemental Text), and yields the same

prediction of a critical worm concentration $w_{tot} = k_{-1}/k_1$ below which no colonies will form.

Thus the model predicts that (i) at steady state, there will be a density threshold, above which one or more colonies form, and below which no colony forms; (ii) when the seeding density is above the colony formation threshold, the density of out-of-colony worms should remain constant; and (iii) the critical colony concentration is equal to the ratio of the association and dissociation rate constants, k_{-1}/k_1. Note that there are only three parameters in the model, the two rate constants and the total density of the worms. In a typical experiment, the density is known, and the rate constants can be directly measured by assessing the rate at which worms enter and leave colonies; therefore, it is possible to quantitatively test the model.

As a first experimental test, we asked whether there is a critical density of worms for colony formation. We placed different initial densities of dauer-stage N2 worms on an agarose plate, gently spread the worms, and took pictures of the plates after 30 min, when the colonies were already stable and no further colonies were forming. In agreement with the model, we found that the out-of-colony worm density increased approximately linearly with the seeding density when the seeding density was below a threshold, and became maximal and constant when the seeding density exceeded the threshold (Fig. 2h, i). The critical density was approximately 1.33 ± 0.25 worms/mm^2 (Fig. 2h, i), estimated by fitting a straight line to the data points where there were no colonies (open circles, Fig. 2i), a flat line to those data points where there were colonies (filled circles, Fig. 2i), calculating the intersection between the two lines, and then averaging over three independent experiments. Thus, colony formation has the hallmarks of a simple condensation process with a transcritical bifurcation.

Next, to test whether the colony-forming threshold can be predicted from k_{-1}/k_1, we took time-lapse videos of worms near existing colonies and measured the association and dissociation rates (Supplementary Movie 3). Note that, according to the model, k_{-1}/k_1 should be a constant and can be measured in a system that has not yet reached the steady state. From several experiments, we calculated the number of association and dissociation events per unit time (as in Eqs. 1 and 2), and calculated

k_{-1}/k_1 by dividing the ratio between the dissociation and the association rates by the density of out-of-colony worms. The critical density threshold predicted from these rate measurements was 1.78 ± 0.17 worms/mm^2, close to the directly-measured threshold of 1.33 ± 0.25 worms/mm^2 (Student's *t*-test *p*-value = 0.303) (Fig. 2j). Thus, a simple condensation model both qualitatively and quantitatively accounts for the worms' behavior.

To further explore the mechanism underpinning colony formation, we hypothesized that much like molecules in a condensed phase, worms in a colony moved more slowly due to their interactions with other worms. To test this hypothesis, we tracked movements of fluorescently-labeled worms sparsely mixed with label-free worms (Supplementary Movie 4). Worms outside of the colony moved six times faster than worms in a colony (Fig. 3a) (Wilcoxon *p*-value < 0.001). This spatially distinct behavioral difference could be a result of (i) two behaviorally differentiated populations of worms, or (ii) a single

population of worms with two behavioral states. To distinguish between these possibilities, we tracked individual worms before and after they transited into or out of a colony. We found that individual worms promptly accelerated upon leaving a colony and decelerated upon joining a colony, supporting the second hypothesis (Fig. 3b, c).

Additionally, chemotaxis or other mechanisms of attraction could contribute to the formation of colonies by increasing the probability of encounter between worms and colonies. To assess the degree of contribution by attraction, we measured the radial and tangential components of velocities of worms at different distances from the center of a colony. If a worm is attracted to a colony, one would expect the radial component to be greater than the tangential component (Fig. 3d). However, we did not see such trend (Wilcoxon *p*-value = 0.73 without distance bins). We also dissected the radial and the tangential components of the velocity by binning the worms according to their distance to a colony (Fig. 3e). At all distances from the colony there was no apparent increase in the radial velocity relative to the tangential velocity, and no significant difference between the speeds of worms moving towards vs. away from the colony (Fig. 3e). This suggests that the worms join colonies through a simple random walk, and then stay in the colony because their movement slows down.

In many inhomogeneous physical-chemical systems, the small-sized structures shrink over time, and eventually disappear, while the large-sized structures grow. This coarsening process is termed Ostwald ripening [18,19]. Ostwald ripening is driven by a greater stability of the larger structures. We have observed a similar phenomenon in *C. elegans* colonies. When there were two or more colonies on the same agarose pad, the small colonies often eventually disappeared. (Fig. 4b). We found that a small modification to the rate equation model (Eq. 5) – adding a colony size-dependent dissociation rate constant – is sufficient to generate Ostwald ripening in the worm model (Fig. 4a; Supplementary Text and Supplementary Fig. 3).

In summary, we have demonstrated that, at high density, *C. elegans* can self-organize and form colonies even in the absence of bacteria. Even though this is a complex behavior exhibited at the level of a group of living organisms, *C. elegans* colony formation can be explained by simple equations like those governing condensation and phase separation. The model predicts a density threshold for colony formation and a constant density of worms out of colonies when the threshold is reached. We found these predictions to be correct through direct experimental observation. With minor adjustments, the model accounts for the phenomenon of Ostwald ripening as well.

Together with other recent work, these observations indicate that biological self-organization and pattern formation, through phase separation, occur across many scales, from molecules [20–23], organelles [2,3], and possibly sub-cellular compartments [24], all the way to a population of organisms.

Methods:

Strains and maintenance. *C. elegans* strains, N2 Bristol and isogenic GFP-labeled GA631, and *E. coli* OP50 were obtained from the Caenorhabditis Genetics Center, University of Minnesota. *C. elegans* were

maintained and cultured routinely on nematode growth (NG) plates according to standard procedures[25].

Liquid culture. To obtain sufficient numbers of *C. elegans*, we cultured *C. elegans* in liquid before experiments. *C. elegans* from a 100 mm plate that had been just depleted of food were washed and transferred to 250 mL S Medium[26] (1 L autoclaved S Basal plus 10 mL 1 M potassium citrate pH 6, 10 mL trace metals solution, 3 mL 1 M $CaCl_2$, 3 mL 1 M $MgSO_4$. S Basal: 5.85 g NaCl, 1 g K_2HPO_4, 6 g KH_2PO_4, 1 mL cholesterol (5 mg/mL in ethanol), H_2O to 1 L; trace metals solution: 1.86 g disodium EDTA, 0.69 g $FeSO_4$•$7H_2O$, 0.2 g $MnCl_2$•$4H_2O$, 0.29 g $ZnSO_4$•$7H_2O$, 0.025 g $CuSO_4$•$5H_2O$, H_2O to 1 L) with 0.5 mL *E. coli* OP50 pellet. To obtain adult worms, cultures were shaken in flasks and incubated at 23 °C for 3 days with monitoring of bacterial density to ensure no starvation of worms. Adults were enriched by transferring cultures to 50 mL Falcon tubes, settled for 5 min, and collected from the bottom. The adults were then washed and settled twice in fresh M9 buffer[26] (3 g KH_2PO_4, 6 g Na_2HPO_4, 5 g NaCl, 1 mL 1 M $MgSO_4$, H_2O to 1 L). To obtain dauer-stage worms, the liquid culture was maintained similarly as for adults except cultured for 10 days. Dauer stage was induced by the high population density in the culture. Worms were transferred to conical 50 mL tubes, and collected from the bottom of tubes after centrifugation at 300 g for 3 min. To remove worms in other developmental stages, worms were then resuspended and incubated in 1% SDS for 40–60 min at room temperature. To separate dauer worms from debris, material was then collected by centrifugation at 300 g for 3 min and followed by centrifugation at 16000 g for 1 min at 4 °C in a tube containing cooled M9 buffer on top and 30% sucrose in M9 buffer at the bottom (sucrose cushion floatation). Dauers were enriched at the interface between the two density layers after centrifugation. These worms were quickly collected with a wide-bore Pasteur pipette and washed twice with M9 buffer at room temperature. Culture density was estimated by counting 20 µL droplets of the purified cultures (or a larger volume if the count is smaller than 50 worms) under a stereoscope.

Colony formation assay on agarose pads. Agarose pads were generated by molding melted 2% agarose (A9539-500G, Millipore-Sigma) in S Medium between two clean glass plates spaced with 1 mm-thick spacers. We used a 7 mm diameter biopsy punch (Queens Surgical) to cut out discs of agarose pads. The pads were then transferred to a 60 mm petri dish (351007, Corning) with a pair of tweezers with carbon fiber tips (159C-RT, Excelta). Worms of desired number were transferred to the top of the agarose pads. Extra liquid was removed using the tip of a piece of Kimwipe (06-666A, Kimberly-Clark) twisted between fingers. The dish was then covered and imaged under a DMi8 fluorescence microscope (Leica).

Colony formation assay on dishes. To make an agarose plate, we dispensed 5 mL 2% agarose with S Medium in a 60 mm petri dish and allowed to solidify. Afterwards, we deposited worms of desired number on to the agarose plate with a pipette. We removed excess liquid and gently dispersed the worms with a soft PVA sponge (40400-8, BVI). The dish was then covered with a lid layered with 2% agarose to reduce condensation and placed on a flatbed scanner (B11B198011, Perfection V600, Epson) for image capture. Scanned photos were taken at 1200 dpi and regular time intervals with a custom Python script.

Image processing and motion tracking. Before segmentation and tracking, a 2D Gaussian kernel was applied to individual images to reduce local fluctuations. The outlines of worms and colonies were generated by thresholding on the edge intensities created by convolution with a Roberts kernel. Object masks for worms and colonies were generated by inversing the binary map of a background flood on the thresholded edge map. Object mask openings of size less than 1,000 μm^2 were removed. We tracked objects by finding the nearest centroid Euclidean neighbor in the previous frame. If the nearest neighbor in the last or the next frame was far enough away that a speed greater than 250 μm/sec would have been required to account for the displacement, the object was considered to be an orphan. Depending on the event sequence and the distance to the edge of the field of view, orphans were classified as entering or exiting a colony or entering or exiting the field of view. Given the uniformity of size of dauer worms, objects were categorized into a worm or a colony by its area of mask opening. Objects containing two worms in two consecutive frames, or algorithmically greater than 1.75 times the area of median opening in the field of view (1.75 times the typical size of a solitary worm) were classified as a colony. Manual inspection was performed to ensure successful implementation.

Declarations

Acknowledgments

We thank Hans Anderson, Sujay Guha, Miriam Goodman and Zhibo Zhang for helpful discussions, and Deborah Gordon, Xianrui Cheng, William Huang, Julia Kamenz, Shixuan Liu, Connie Phong for comments on the manuscript. This work was supported by a grant from the National Institutes of Health (R35 GM131792). Some strains were provided by the CGC, which is funded by NIH Office of Research Infrastructure Programs (P40 OD010440).

Competing interests:

Authors declare no competing interests.

Data and materials availability

All data, code, and materials used in the analysis are available to any researcher for purposes of reproducing or extending the analysis.

Author contributions:

Conceptualization: Y.C. and J.E.F.; Formal analysis: Y.C.; Funding acquisition: J.E.F.; Investigation: Y.C.; Supervision: J.E.F.; Visualization: Y.C. and J.E.F.; Writing: Y.C. and J.E.F.; Editing: Y.C. and J.E.F.

References

1. Banani, S. F., Lee, H. O., Hyman, A. A. & Rosen, M. K. Biomolecular condensates: organizers of cellular biochemistry. *Nat Rev Mol Cell Biol* **18**, 285–298, doi:10.1038/nrm.2017.7 (2017).
2. Brangwynne, C. P. *et al.* Germline P granules are liquid droplets that localize by controlled dissolution/condensation. *Science* **324**, 1729–1732, doi:10.1126/science.1172046 (2009).
3. Molliex, A. *et al.* Phase separation by low complexity domains promotes stress granule assembly and drives pathological fibrillization. *Cell* **163**, 123–133, doi:10.1016/j.cell.2015.09.015 (2015).
4. Feric, M. *et al.* Coexisting Liquid Phases Underlie Nucleolar Subcompartments. *Cell* **165**, 1686–1697, doi:10.1016/j.cell.2016.04.047 (2016).
5. Larsch, J. *et al.* A Circuit for Gradient Climbing in C. elegans Chemotaxis. *Cell Rep* **12**, 1748–1760, doi:10.1016/j.celrep.2015.08.032 (2015).
6. Zhang, Y., Lu, H. & Bargmann, C. I. Pathogenic bacteria induce aversive olfactory learning in Caenorhabditis elegans. *Nature* **438**, 179–184, doi:10.1038/nature04216 (2005).
7. Artyukhin, A. B., Yim, J. J., Cheong Cheong, M. & Avery, L. Starvation-induced collective behavior in C. elegans. *Sci Rep* **5**, 10647, doi:10.1038/srep10647 (2015).
8. Sugi, T., Ito, H., Nishimura, M. & Nagai, K. H. C. elegans collectively forms dynamical networks. *Nat Commun* **10**, 683, doi:10.1038/s41467-019-08537-y (2019).
9. de Bono, M. & Bargmann, C. I. Natural variation in a neuropeptide Y receptor homolog modifies social behavior and food response in C. elegans. *Cell* **94**, 679–689, doi:10.1016/s0092-8674(00)81609-8 (1998).
10. Zimmer, M. *et al.* Neurons detect increases and decreases in oxygen levels using distinct guanylate cyclases. *Neuron* **61**, 865–879, doi:10.1016/j.neuron.2009.02.013 (2009).
11. Gray, J. M. *et al.* Oxygen sensation and social feeding mediated by a C. elegans guanylate cyclase homologue. *Nature* **430**, 317–322, doi:10.1038/nature02714 (2004).
12. Demir, E., Yaman, Y. I., Basaran, M. & Kocabas, A. Dynamics of pattern formation and emergence of swarming in C. elegans. *Elife* **9**, e52781, doi:10.7554/eLife.52781 (2020).
13. Gray, J. M., Hill, J. J. & Bargmann, C. I. A circuit for navigation in Caenorhabditis elegans. *Proc Natl Acad Sci U S A* **102**, 3184–3191, doi:10.1073/pnas.0409009101 (2005).
14. Strogatz, S. *Nonlinear Dynamics And Chaos: With Applications To Physics, Biology, Chemistry, And Engineering (Studies in Nonlinearity)*. (Westview Press, 2001).
15. Hyman, A. A., Weber, C. A. & Jülicher, F. Liquid-Liquid Phase Separation in Biology. *Annual Review of Cell and Developmental Biology* **30**, 39–58, doi:10.1146/annurev-cellbio-100913-013325 (2014).
16. Israelachvili, J. N., Mitchell, D. J. & Ninham, B. W. Theory of self-assembly of hydrocarbon amphiphiles into micelles and bilayers. *Journal of the Chemical Society, Faraday Transactions 2: Molecular and Chemical Physics* **72**, 1525–1568, doi:10.1039/F29767201525 (1976).
17. Tanford, C. *The hydrophobic effect: formation of micelles and biological membranes*. (Wiley, 1973).

18. 10.1515/zpch-1897-2233
Ostwald, W. Studien über die Bildung und Umwandlung fester Körper. *Zeitschrift für Physikalische Chemie* **22U**, 289–330, doi:10.1515/zpch-1897-2233 (1897).
19. Voorhees, P. W. The theory of Ostwald ripening. *Journal of Statistical Physics* **38**, 231–252, doi:10.1007/bf01017860 (1985).
20. Huang, W. Y. C. *et al.* A molecular assembly phase transition and kinetic proofreading modulate Ras activation by SOS. *Science* **363**, 1098–1103, doi:10.1126/science.aau5721 (2019).
21. Lin, Y., Protter, D. S., Rosen, M. K. & Parker, R. Formation and Maturation of Phase-Separated Liquid Droplets by RNA-Binding Proteins. *Mol Cell* **60**, 208–219, doi:10.1016/j.molcel.2015.08.018 (2015).
22. Su, X. *et al.* Phase separation of signaling molecules promotes T cell receptor signal transduction. *Science* **352**, 595–599, doi:10.1126/science.aad9964 (2016).
23. Elbaum-Garfinkle, S. *et al.* The disordered P granule protein LAF-1 drives phase separation into droplets with tunable viscosity and dynamics. *Proc Natl Acad Sci U S A* **112**, 7189–7194, doi:10.1073/pnas.1504822112 (2015).
24. Cheng, X. & Ferrell, J. E., Jr. Spontaneous emergence of cell-like organization in Xenopus egg extracts. *Science* **366**, 631–637, doi:10.1126/science.aav7793 (2019).
25. S. Brenner, The genetics of *Caenorhabditis elegans*. *Genetics* 77, 71–94 (1974).
26. T. Stiernagle, in *WormBook*, T. C. e. R. Community, Ed. (2006).
27. T. Nishinaga, *Handbook of Crystal Growth: Fundamentals*. Handbook of Crystal Growth (Elsevier Science, 2014).

Supplemental Videos

Supplemental videos are not available with this version.

Figures

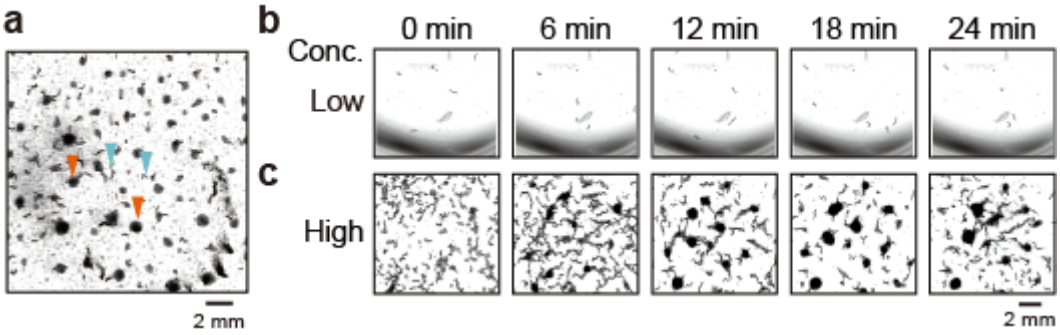

Figure 1

C. elegans form colonies at high density in the absence of bacteria. a N2 C. elegans formed colonies on an NG plate upon consumption of bacteria. Orange arrowheads: colonies; blue arrowheads: dispersed

worms. b, c Washed adult N2 C. elegans seeded at a low concentration (0.01 worms/mm2) (b) did not form stable colonies on an agarose plate, but those seeded at high density (0.18 worms/mm2) (c) did.

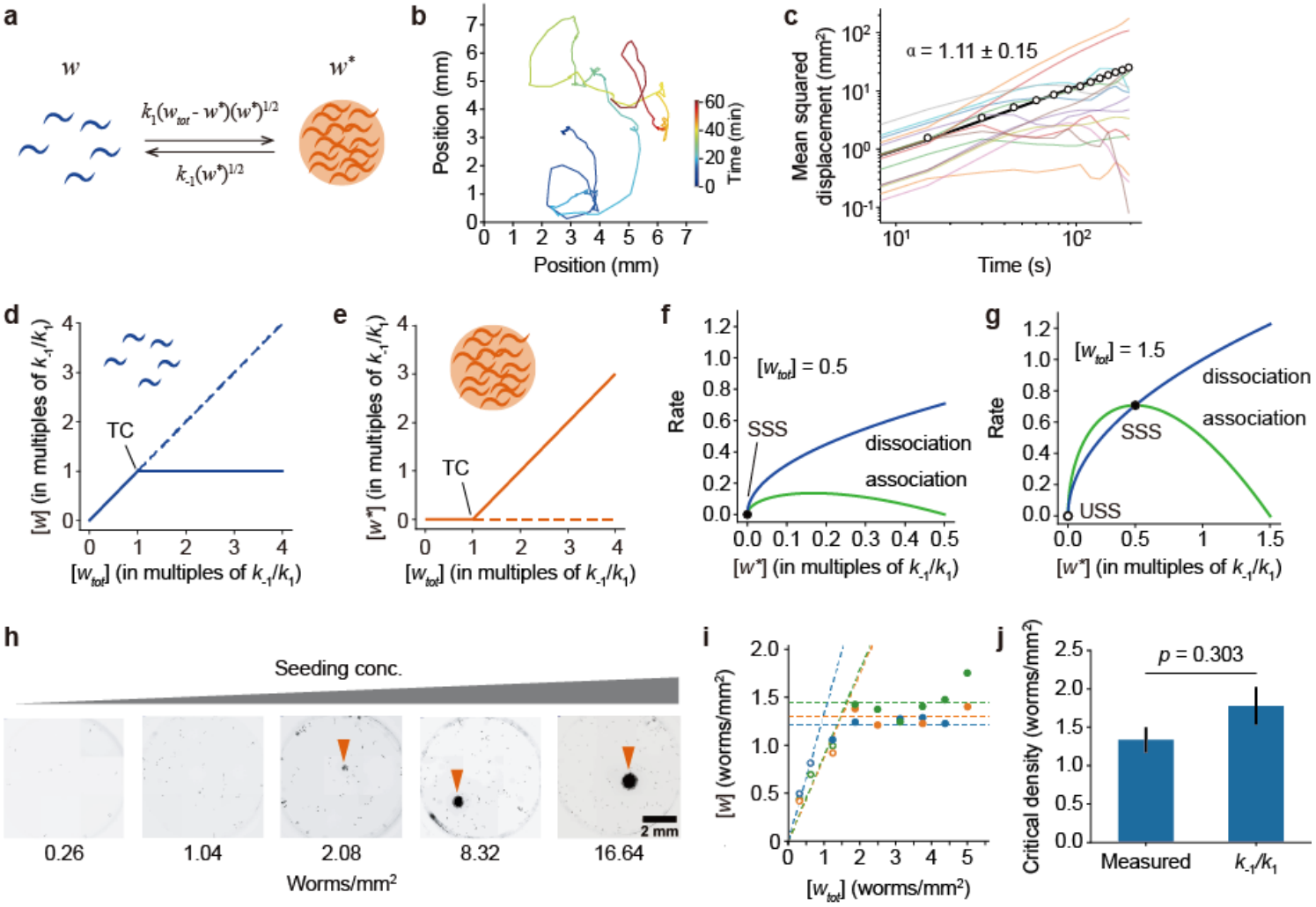

Figure 2

C. elegans colony formation is a condensation process. a Schematic of the rate equation model for colony formation. b Sample trajectory of a single worm. c, d The modeled steady-state densities of worms out of colonies (w), and in one or more colonies (w*), as a function of the total density of worms wtot, based onto Eqs. 7 and 8. The system has a single stable steady state until the concentration of worms reaches a critical value of wtot = k-1/k1 (TC, transcritical bifurcation point). Beyond the critical density, the system bifurcates, and has an unstable steady state (dashed) and a stable steady state (solid) with a constant density of the dispersed worms w. e, f Rate balance analysis of a case with wtot smaller than the critical density (wtot = 0.5k1/k-1), and one with wtot greater than the critical density (wtot = 1.5k1/k-1). The association (green) and dissociation (blue) rates intersect at the steady states. In (e), the single steady state is stable (SSS), as small perturbations make dissociation faster than association, making the system return toward the steady state. In (f), the steady state at w* = 0 is unstable (USS), as small perturbation would make association faster than dissociation, and drive the system away from that steady state. g Dauer stage worms were seeded at various densities on agarose pads and the system was allowed to equilibrate for 30 min. Colonies appeared on pads with higher

seeding density (arrows) but not with lower. h Measured densities of dispersed worms as a function of seeding density. Dauer stage worms were seeded at various densities on agarose plates and the system was allowed to equilibrate for 30 min. Plates where colonies formed are indicated with filled circles, and plates with no colonies with open circles. Data are from three independent experiments. i Critical density measured directly as in (h) (mean ± S.E.M., n = 3) and compared to predicted critical density values obtained by measuring k-1 and k1 from time-lapse movies of dauer stage worms (not necessarily at steady state) (n = 7). The p-value was calculated using Student's t-test.

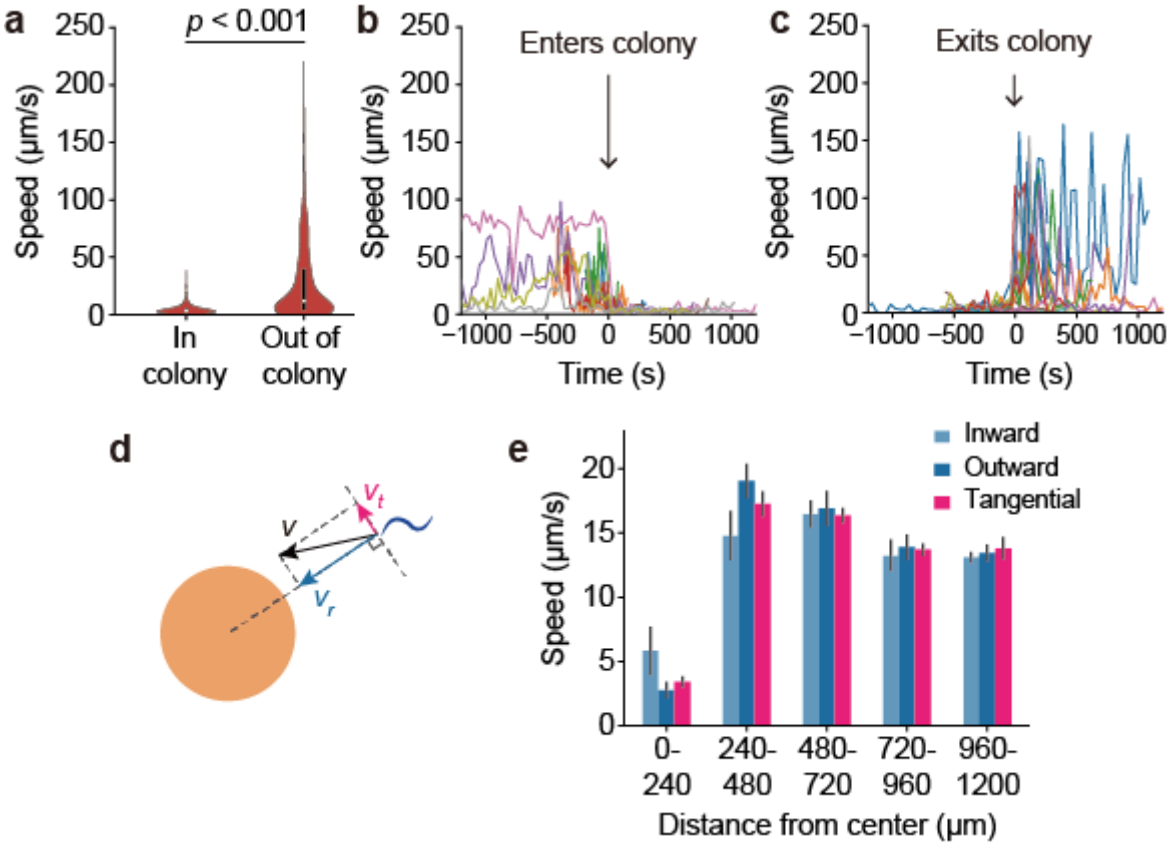

Figure 3

Difference in speed drives C. elegans colony formation. a A violin plot of the speeds of worms in colonies and outside of colonies. The black bars span the 25th to 75th percentiles. Open circles indicate median values. The Wilcoxon rank-sum test p-value is shown (n = 769 on colony; 1378 out of colony). b, c examples of worms slowing down upon entering a colony (b) and speeding up upon exiting a colony (c). d Schematic of breaking down a worm's velocity into radial and tangential components. A colony is shown as an orange disc, and a worm as a blue curl. The radial component of the velocity is shown as a blue arrow, and tangential shown as magenta arrow. e Measured radial and tangential velocities for worms at various distances from a colony. Most of the worms in the first bin were in colonies. Ten colonies from two independent experiments were included in the analysis. Velocity components were averaged for each colony at each distance before statistical analysis. Error bars are standard errors of the mean.

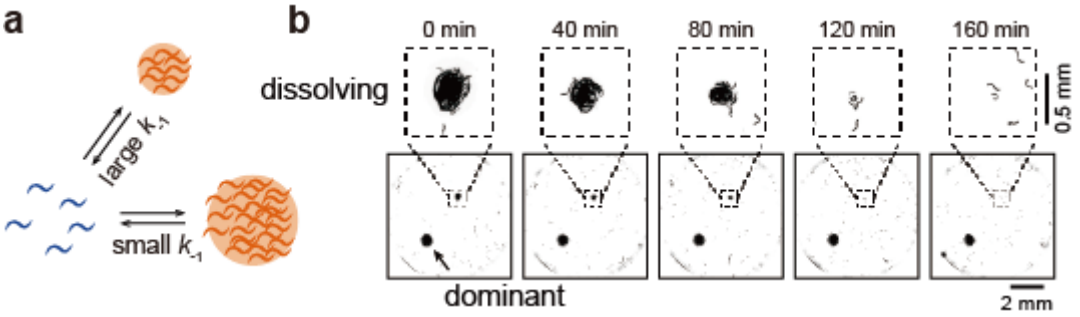

Figure 4

Ostwald ripening in C. elegans colony formation. a A simple model for Ostwald ripening, where the k-1 value is assumed to decrease with colony size. b An example of a small colony that progressively decreases in size and then disappears.

Supplementary Files

This is a list of supplementary files associated with this preprint. Click to download.

- 071620WormSupplementaryNatCommFormat.docx